Supporting Information for

A Comparative Study of the Photophysics of Phenyl, Thienyl, and Chalcogen Substituted Rhodamine Dyes

Randy P. Sabatini †, Michael F. Mark †, Daniel J. Mark †, Mark W. Kryman ‡, Jacqueline E. Hill ‡, William W. Brennessel, Michael R. Detty ‡*, Richard Eisenberg †*, David W. McCamant †*

†Department of Chemistry, University of Rochester, Rochester, New York 14627, United States

‡Department of Chemistry, University at Buffalo, The State University of New York, Buffalo, New York 14260, United States

Table of Contents

Synthesis of **S-Pyr**, **Se-Pyr**, and **S-Th-5-PO(OEt)$_2$**

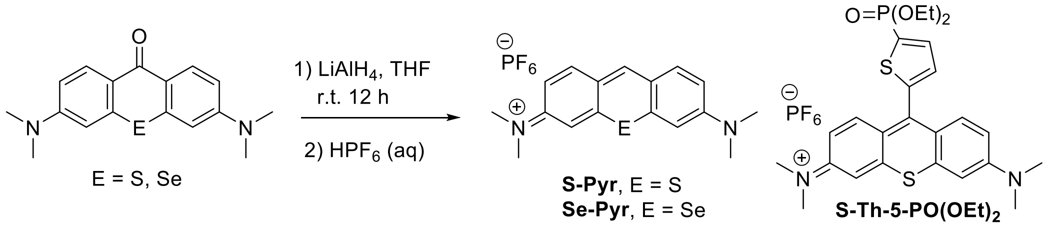

Se-Pyr:

Lithium aluminum hydride (33 mg, 0.869 mmol, 3.0 eq) was added to a stirred solution of Se-xanthone[1] (100mg, 0.290 mmol, 1.0 eq) and the resulting solution was stirred at ambient temperature for 12 h. The reaction was quenched by the slow addition of aqueous 5% HPF_6 (2 mL) and the resulting mixture was poured into 100 mL of aqueous 10% HPF_6. After stirring for 12 h, the precipitate was collected via filtration and washed with water (50 mL) and diethyl ether (4 x 25 mL). The crude product was recrystallized from acetonitrile to give 90 mg (65%) of **Se-Pyr** as a dark green solid, m.p. ^{1}H NMR (500 MHz, CD_2Cl_2:CD_3CN) δ 8.22 (s, 1 H), 7.94 (d, 1 H, *J* = 10.0 Hz), 7.24 (d, 1 H, *J* = 2.0 Hz), 7.06 (d x d, 1 H, *J* = 9.0, 2.0), 3.29 (s, 12 H); HRMS (ESI) *m/z* 331.0708 (calcd for $C_{17}H_{19}N_2{}^{80}Se$: 331.0708); λ_{max} in CH_2Cl_2 (ε, M^{-1} cm^{-1}) 571 nm (1.26 x 10^5), λ_{max} in MeOH (ε, M^{-1} cm^{-1}) 567 nm (9.20 x 10^4), mp = 248-250 °C.

S-Pyr:

Lithium aluminum hydride (42 mg, 1.01 mmol, 3.0 eq) was added to a stirred solution of S-xanthone[1] (100 mg, 0.335 mmol, 1.0 eq) and the resulting solution was stirred at ambient temperature for 12 h. The reaction was quenched by the slow addition of aqueous 5% HPF_6 (2 mL) and the resulting mixture was poured into 100 mL of aqueous 10% HPF_6. After stirring for 12 h, the precipitate was collected via filtration and washed with water (30 mL) and diethyl ether (4 x 25 mL). The crude dye was recrystallized in acetonitrile to give 23 mg (16%) of **S-Pyr** as a green solid, m.p. ^{1}H NMR (500 MHz, CH_2Cl_2) δ 8.33 (s, 1 H), 7.91 (d, 2 H, *J* = 9 Hz), 7.13 (d x d, 2 H, *J* = 9.5, 2.5 Hz), 7.07 (s, 2 H), 3.31 (s, 12 H); HRMS (ESI) *m/z* 283.1263 (calcd for $C_{17}H_{19}N_2S^+$: 283.1263); λ_{max} (CH_2Cl_2) 563 nm (ε = 1.24 x 10^5 $M^{-1}cm^{-1}$), λ_{max} (CH_3OH) 559 nm (ε = 8.86 x 10^4 $M^{-1}cm^{-1}$), mp = 254-257 °C.

S-Th-5-PO(OEt)$_2$:

The literature procedure[2] described for the synthesis of **O-Th-5-PO(OEt)$_2$** and **Se-Th-5-PO(OEt)$_2$** was followed to prepare **S-Th-5-PO(OEt)$_2$**. *n*-Butyllithium (1.55 M in hexanes, 1.48 mL, 2.30 mmol) was added dropwise to a stirred solution of thiophene (0.184 mL, 2.30 mmol) and *N,N,N′,N′*-tetramethylethylenediamine (0.347 mL, 2.30 mmol) in 50 mL of anhydrous anhydrous tetrahydrofuran (THF) at –78 °C. After 25 min, the resulting solution was transferred via cannula to a solution of diethyl phosphorochloridate (0.332 mL, 2.30 mmol) dissolved in 5 mL of THF at ambient temperature. The resulting mixture was heated at 50 °C for 15 min and then cooled again to –78 °C. A solution of LDA prepared from diisopropylamine (0.357 mL, 2.53 mmol) and *n*-butyllithium (1.55 M in hexanes, 1.48 mL, 2.30 mmol) in 5 mL of anhydrous THF was added. The resulting mixture was stirred 5 min at –78 °C before the mixture was transferred via cannula to a stirred solution of S-xanthone[1] (229 mg, 0.767 mmol) dissolved in 5 mL of anhydrous THF at ambient temperature. The resulting mixture was heated at 50 °C for 30 min. Acetic acid (1 mL) was added, and the resulting mixture was poured into a 10% v/v solution of stirred, cold, aqueous HPF_6 (50 mL). After 1 h, the precipitate was collected and washed with water (5 mL) and diethyl ether (5 mL). The product was purified via column chromatography (SiO_2, 10% diethyl ether/CH_2Cl_2 followed by 10% MeOH/CH_2Cl_2. The product-containing fractions were concentrated under reduced pressure yielding 304 mg (61%) of dark blue crystals, mp 227–229 °C. ^{1}H NMR (500 MHz, CD_3CN) δ 7.77 (dd, 1 H, *J* = 3.5, 9.0 Hz), 7.53 (d, 2 H, *J* = 10 Hz), 7.35 (t, 1 H, *J* = 3.5), 7.22 (d, 2 H, *J* = 2.5 Hz), 7.06 (dd, 2 H, *J* = 2.5, 10 Hz), 4.19 (m, 4 H), 3.24 (s, 12 H), 1.34 (t, 6 H, *J* = 7.5 Hz); ^{13}C NMR (125.7 MHz, CD_3CN) δ 154.6, 145.9, 144.7, 138.3, 137.4 (d, *J* = 10.4 Hz), 136.4, 133.0 (d, *J* = 17.3 Hz), 120.3, 116.8, 110.1, 106.7, 64.0 (d, *J* = 5.8 Hz), 16.7 (d, *J* = 5.8 Hz); λ_{max} (CH_2CN) 618 nm (⍰ = 6.1×10^4 M^{-1} cm^{-1}); HRMS (EI) *m/z* 501.1430 (calcd for $C_{29}H_{27}O_3N_2PS_2^+$: 501.1430).

Further details on the synthesis of O/S/Se-Th-5-CO_2H:

An error in publication eliminated some important structures in ref. 35 in the main text (Gannon and Detty, *J.Org. Chem.* **2007**, *72*, 2647.). The synthetic details in Reference 35 refer to the following structures for the xanthones and dyes **O-Th-5-CO_2H**, **S-Th-5-CO_2H**, and **Se-Th-5-CO_2H**:

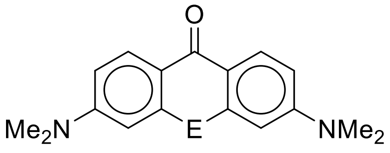

2, E = O, S, Se

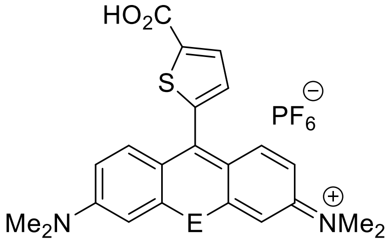

7, E = O
8, E = S
9, E = Se

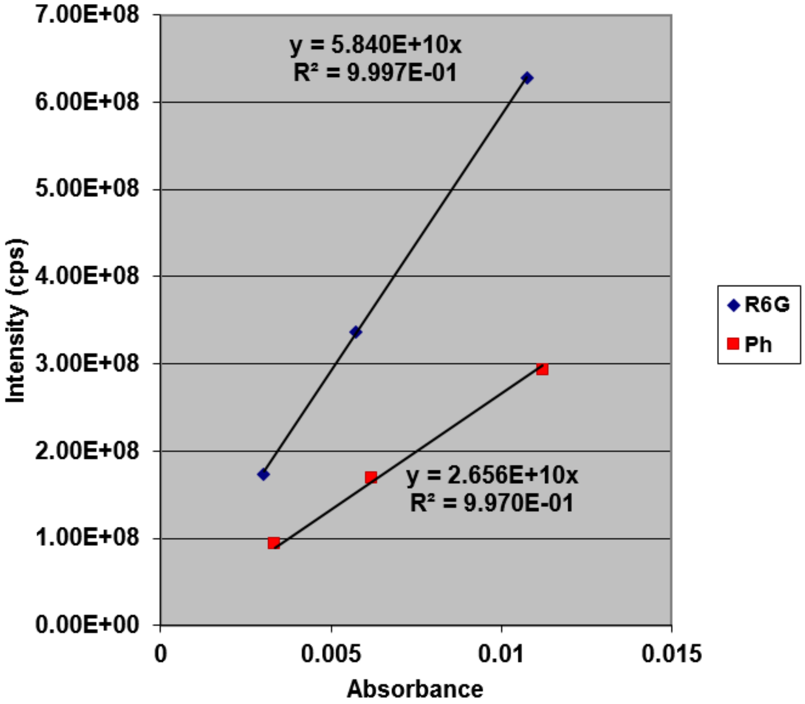

Figure S1: Plots of area of fluorescence intensity versus absorption at wavelength of excitation for **O-Ph** and standard Rhodamine 6G. The other quantum yield values were measured in the same way against their respective standards.

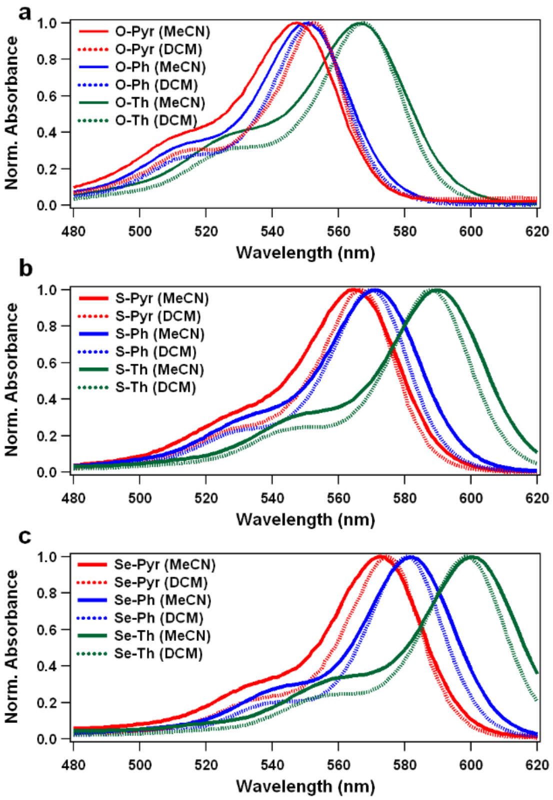

Figure S2: (a) Absorption spectra of **O-Pyr**, **O-Ph**, and **O-Th** in MeCN and CH_2Cl_2 . (b) Absorption spectra of **S-Pyr**, **S-Ph**, and **S-Th** in MeCN and CH_2Cl_2 . (c) Absorption spectra of **Se-Pyr**, **Se-Ph**, and **Se-Th** in MeCN and CH_2Cl_2 .

Crystallography

Crystal structures for dyes **O-Ph** and **O-Th** were obtained in this work. Structures have been deposited in the Cambridge Crystallographic Data Centre, CCDC 1446523-1446524. In structure **O-Ph**, the asymmetric unit contains one cation and one anion in general positions. The pendant phenyl ring is modeled as disordered over two positions (0.57:0.43). Off-center parallel pi-stacking motifs link molecules in columns throughout the crystal with alternating planar distances of approximately 3.3 and 3.4 Å. The angle between the plane of the fused rings and that of the pendant phenyl ring is 59.8(2) degrees. In structure **O-Th**, the asymmetric unit contains one cation and one anion in general positions. The pendant thiophenyl ring is modeled as disordered over two positions (0.81:0.19). Off-center parallel pi-stacking links alternating inverted molecules along the [001] direction with planar distances of approximately 3.5 Å. The angle between the plane of the fused rings and that of the major orientation pendant thiophenyl ring is 49.3(4) degrees. In structure **O-Th**, two pocket volumes per unit cell, located at crystallographic inversion centers, contained highly disordered solvent (likely methanol). Reflection contributions from these solvent volumes were fixed and then added to the calculated structure factors using the Squeeze function of program *PLATON*,[3] which determined there to be 81 electrons in 263 Å^3 accounted for. Because the exact identity and amount of solvent are unknown, no solvent was included in the atom list or the molecular formula. Thus all calculated quantities that derive from the molecular formula (e.g., F(000), molecular weight, density, etc.) are known to be incorrect. See Table S1 for additional details.

Table S1: Crystal data summary for structures **O-Ph** and **O-Th**.

	O-Ph	**O-Th**[a]
Formula	$C_{23}H_{23}F_6N_2OP$	$C_{21}H_{21}F_6N_2OPS$
fw	488.40	494.43
T (K)	100.0(5)	100.0(5)
cryst syst	monoclinic	monoclinic
space group	$P2_1/c$	$P2_1/c$
a (Å)	8.1397(9)	15.031(2)
b (Å)	15.2283(16)	21.396(3)
c (Å)	18.0213(19)	7.4045(11)
β (deg)	102.251(2)	102.883(3)
V (Å^3)	2182.9(4)	2321.3(6)
Z	4	4
ρ_{calcd} (g cm^{-3})	1.486	1.415
μ (mm^{-1})	0.196	0.272
color, shape	red-blue, block	yellow-violet, needle
reflns collected	57048	23326
reflns independent	11919	4105

R_{int}[b]	0.0400	0.0988
reflns observed	8314	2636
number of parameters	321	307
GOF[c] on F^2	1.037	1.014
$R1$ $[I > 2\sigma(I)]$[d]	0.0524	0.0523
$wR2$[e] (all data)	0.1622	0.1289

[a] An unknown amount of solvent is not included in this structure's calculated quantities; see *Experimental* section. [b] $R_{int} = \Sigma |F_o^2 - \langle F_o^2 \rangle| / \Sigma F_o^2$. [c] $GOF = S = [\Sigma w(F_o^2 - F_c^2)^2 / (m - n)]^{1/2}$, where $w = 1 / [\sigma^2(F_o^2) + (aP)^2 + bP]$, P = 1/3 max $(0, F_o^2) + 2/3F_c^2$, m = number of independent reflections, and n = number of parameters. [d] $R1 = \Sigma ||F_o| - |F_c|| / \Sigma |F_o|$. [e] $wR2 = [\Sigma w(F_o^2 - F_c^2)^2 / \Sigma wF_o^2]^{1/2}$.

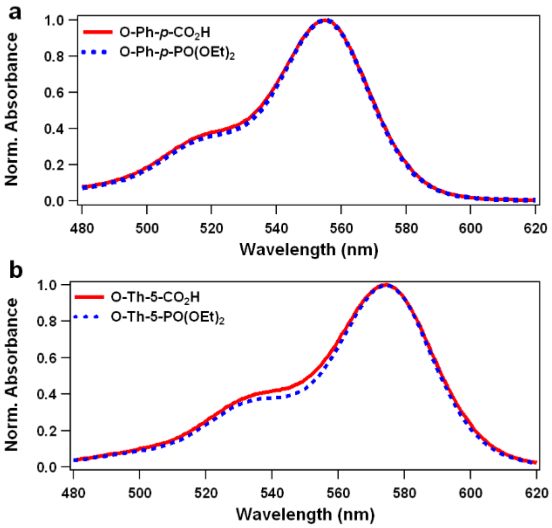

Figure S3: (a) Absorption spectra of **O-Ph-*p*-R**. (b) Absorption spectra of **O-Th-5-R**. No real change is seen when substituting out a carboxylic acid group for a phosphonate ester group.

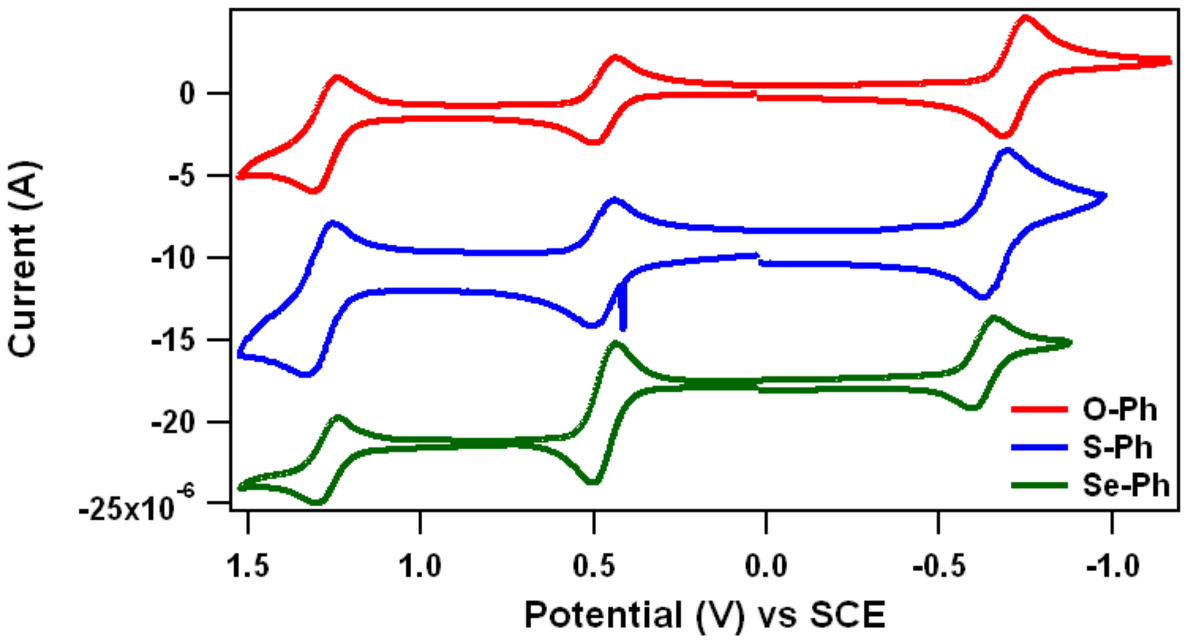

Figure S4: Cyclic voltammograms of series **E-Ph** with different chalcogens.

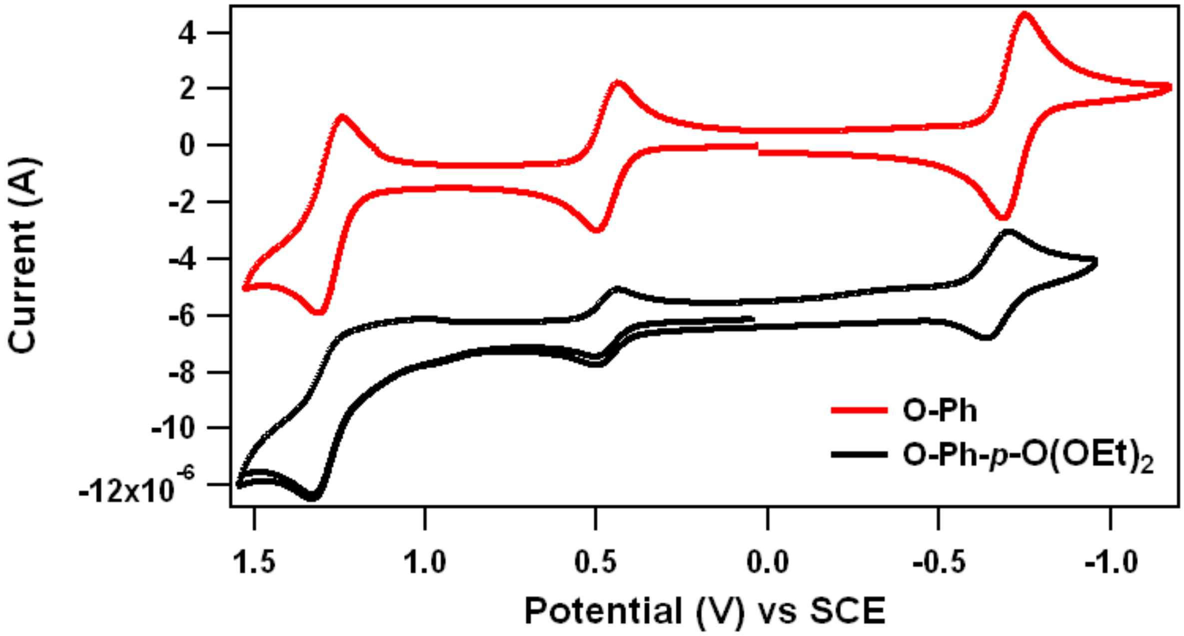

Figure S5: Cyclic voltammograms of **O-Ph** and **O-Ph-*p*-PO(OEt)$_2$.**

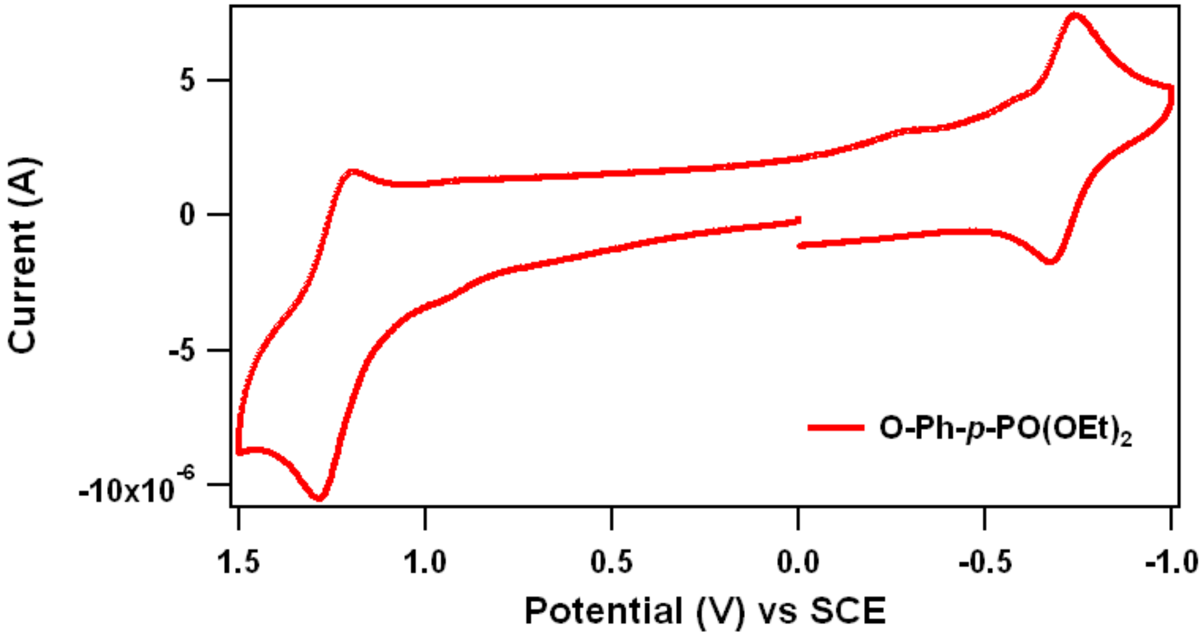

Figure S6: Cyclic voltammogram of **O-Ph-*p*-PO(OEt)$_2$** at a scan rate of 1V/s. This was used to determine the half wave potential of the oxidation.

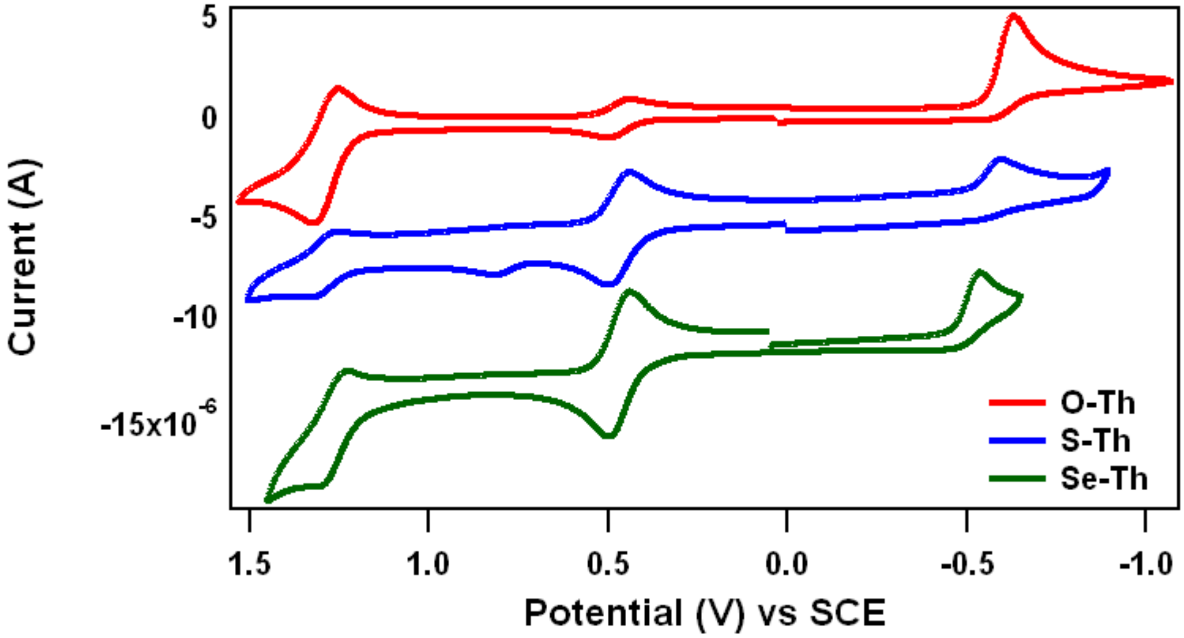

Figure S7: Cyclic voltammograms of series **E-Th** with different chalcogens.

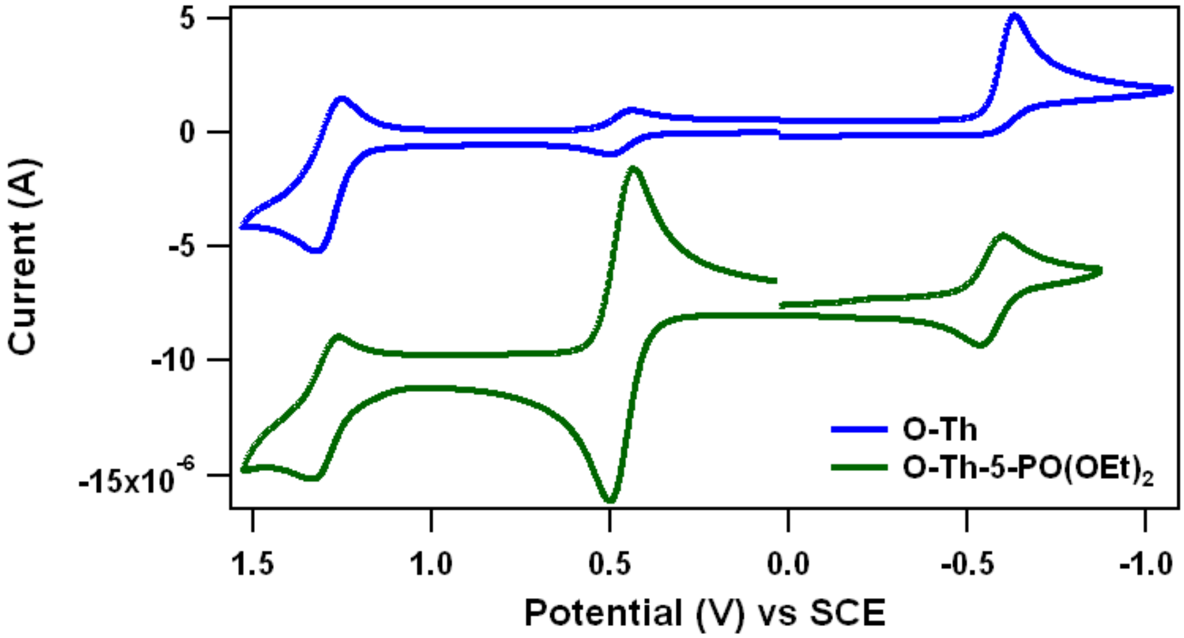

Figure S8: Cyclic voltammograms of **O-Th** and **O-Th-5-PO(OEt)$_2$**.

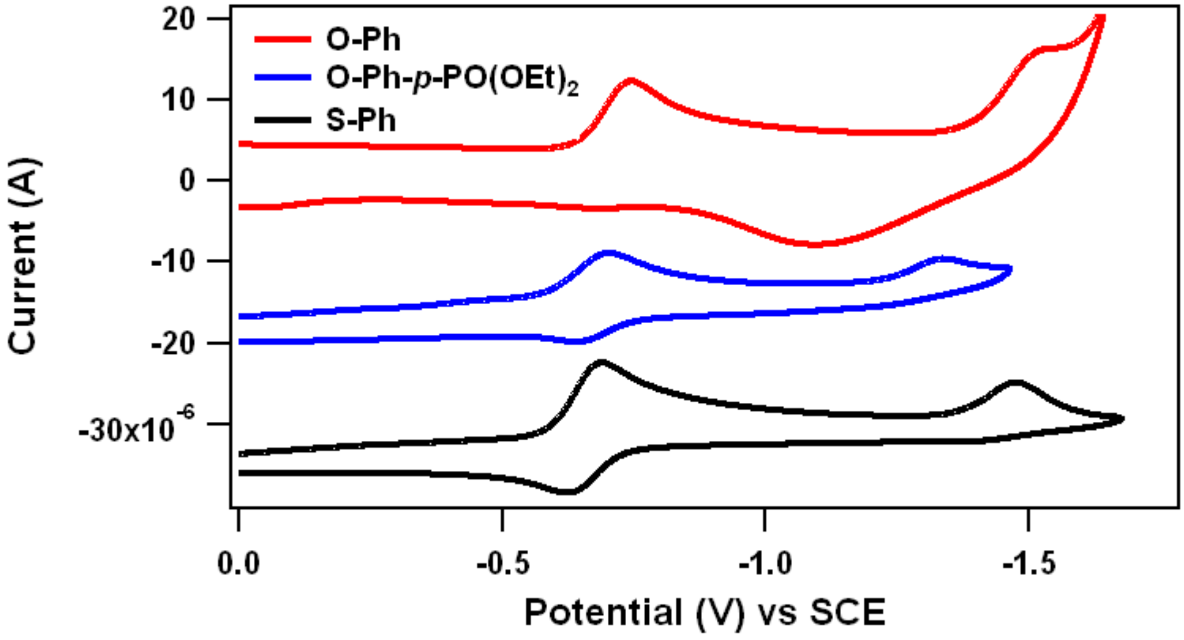

Figure S9: 1st and 2nd reduction waves of **O-Ph**, **O-Ph-*p*-PO(OEt)$_2$**, and **S-Ph**.

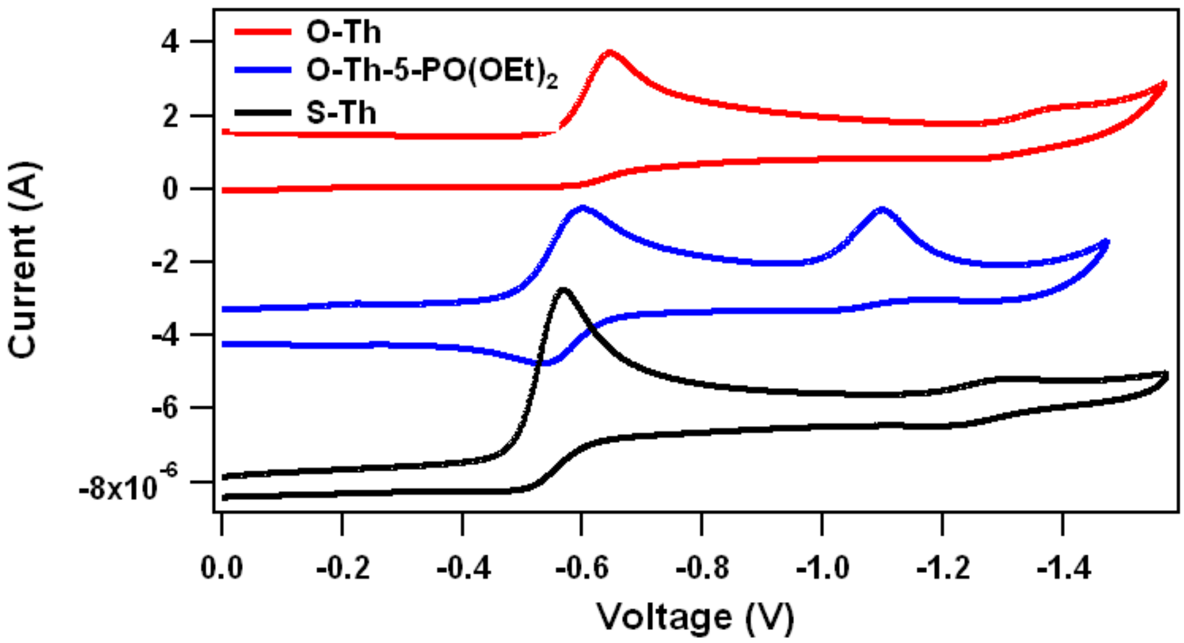

Figure S10: 1st and 2nd reduction potentials of **O-Th**, **O-Th-5-PO(OEt)$_2$**, and **S-Th**.

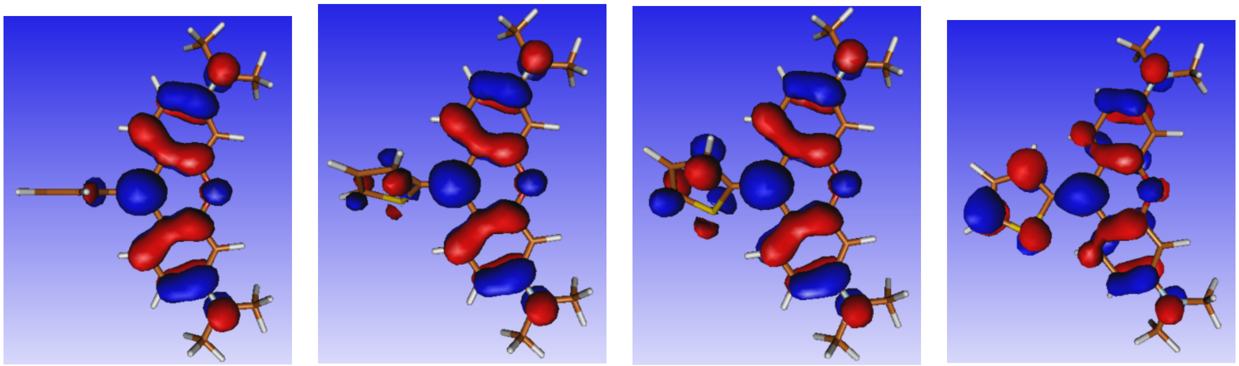

Figure S11: LUMO orbital of **O-Th** with different held thienyl – xanthylium dihedral angles. 90° on left, to 60°, 30°, and 0° on right.

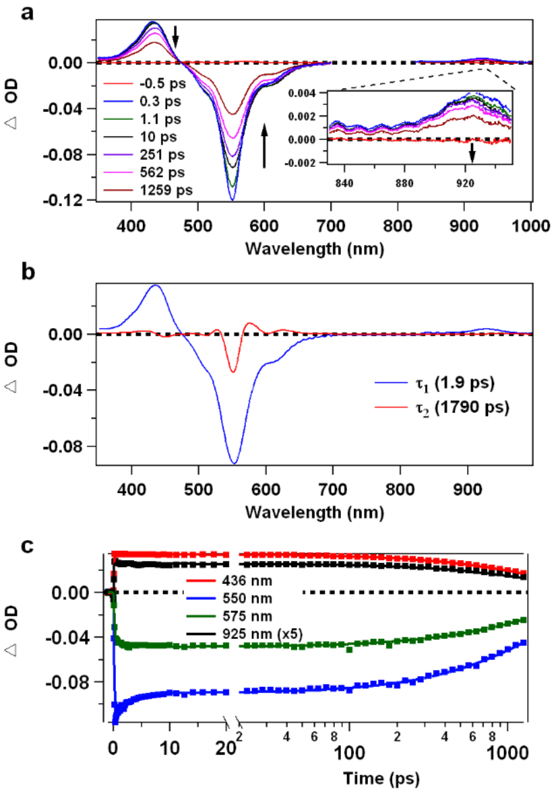

Figure S12: (a) Transient absorption spectra of **O-Pyr** in MeOH. (b) EAS of **O-Pyr** in MeOH. (c) Kinetics of **O-Pyr** in MeOH.

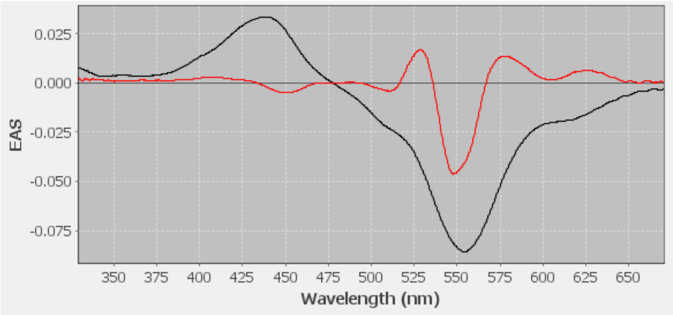

Figure S13: EAS of **O-Pyr** in MeCN. Red = 0.45 ps, Black = 1963 ps

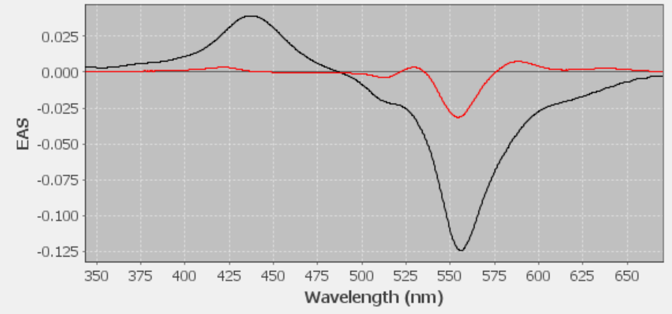

Figure S14: EAS of **O-Pyr** in CH_2Cl_2 . Red = 0.91 ps, Black = 3610 ps

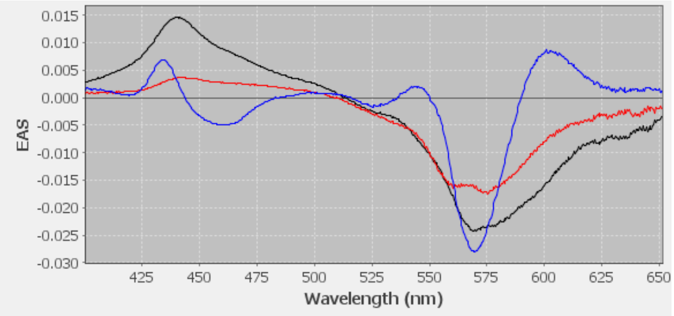

Figure S15: EAS of **S-Pyr** in MeCN. Blue= 0.45 ps, Black = 2242 ps, Red = triplet state (the apperance of SE in triplet state is an artifact of low signal and fitting long time constants using a 1 ns experiment)

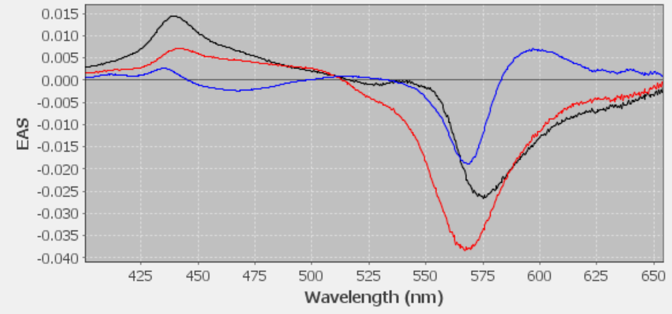

Figure S16: EAS of **S-Pyr** in CH_2Cl_2 . Blue = 0.62 ps, Black = 2794 ps, Red = triplet state (the presence of SE in triplet state is an artifact of fitting long time constants using a 1 ns experiment)

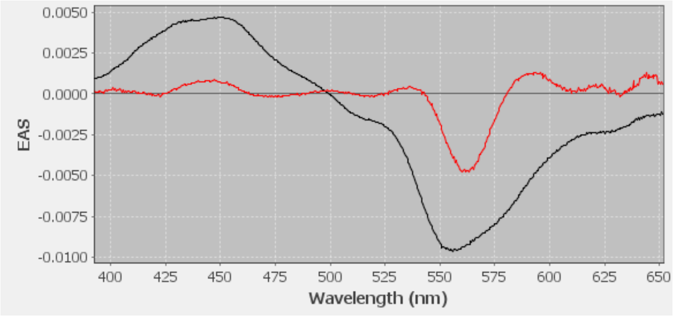

Figure S17: EAS of **O-Ph** in MeCN. Red = 0.43 ps, Black = 2111 ps

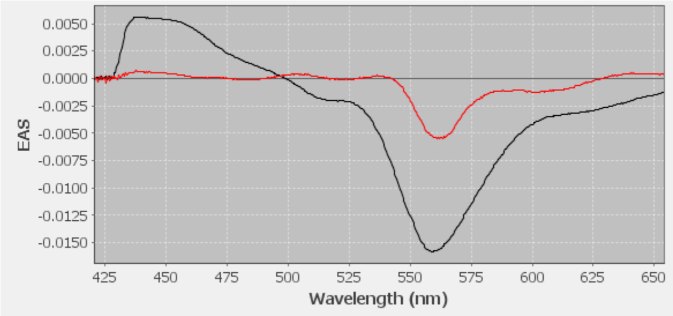

Figure S18: EAS of **O-Ph** in CH_2Cl_2 . Red = 0.96 ps, Black = 3849 ps

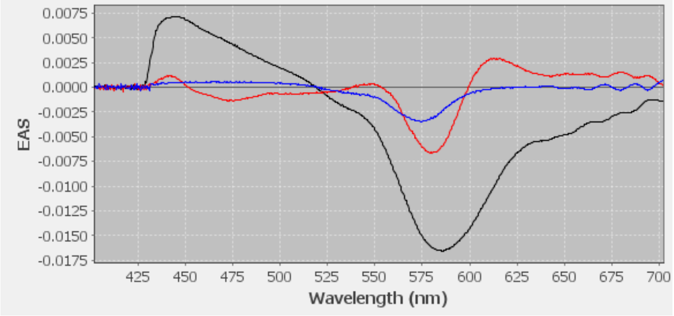

Figure S19: EAS of **S-Ph** in MeCN. Red = 0.35 ps, Black = 1772 ps, Blue = triplet state

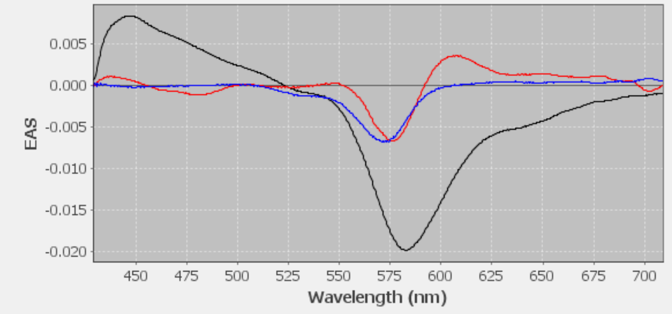

Figure S20: EAS of **S-Ph** in CH_2Cl_2 . Red = 0.47 ps, Black = 2095 ps, Blue = triplet state

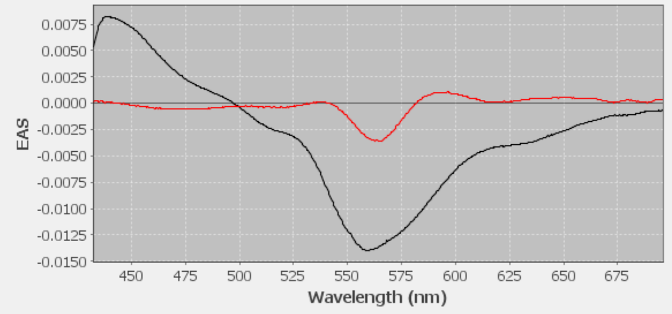

Figure S21: EAS of **O-Ph-*o*-CO_2H** in acidified MeCN. Red = 0.49 ps, Black = 2465 ps

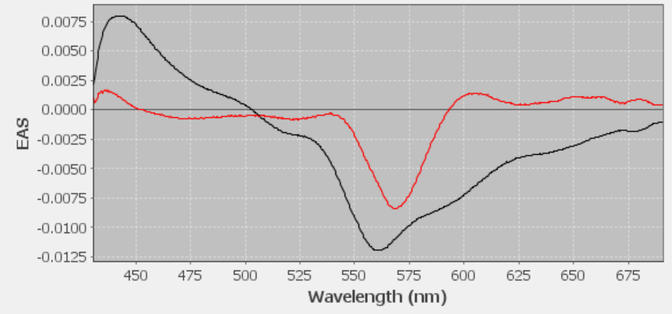

Figure S22: EAS of **O-Ph-*p*-CO_2H** in acidified MeCN. Red = 0.36 ps, Black = 1769 ps

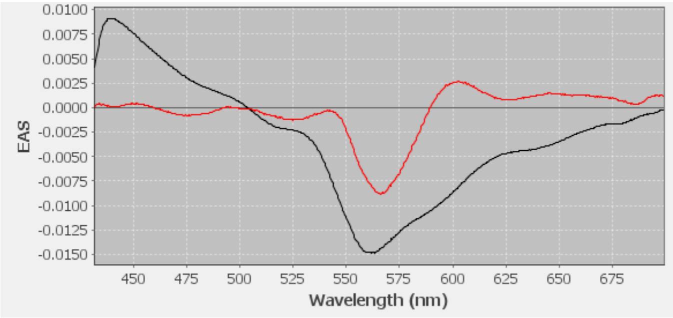

Figure S23: EAS of **O-Ph-*p*-PO(OEt)$_2$** in MeCN. Red= 0.35 ps, Black = 2126 ps

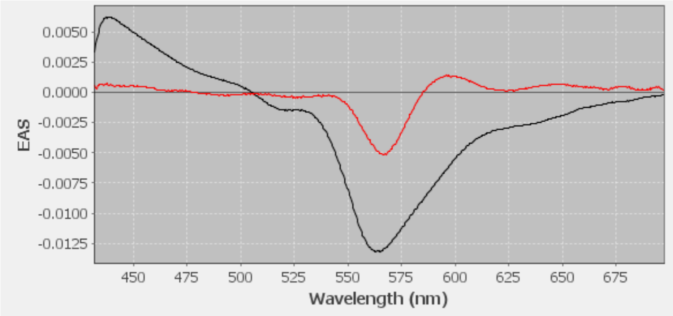

Figure S24: EAS of **O-Ph-*p*-PO(OEt)$_2$** in CH_2Cl_2 . Red = 0.8 ps, Black = 3494 ps

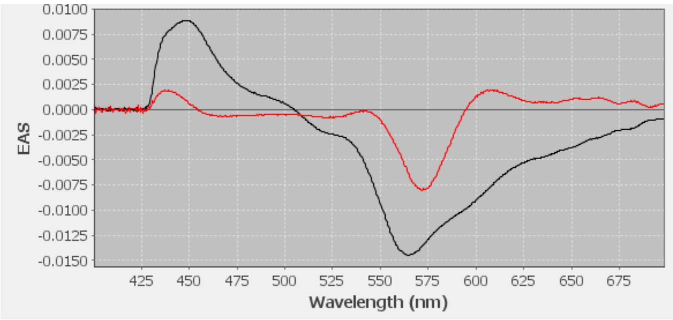

Figure S25: EAS of **O-Th-2-CO$_2$H** in acidified MeCN. Red = 0.53 ps, Black = 2747 ps

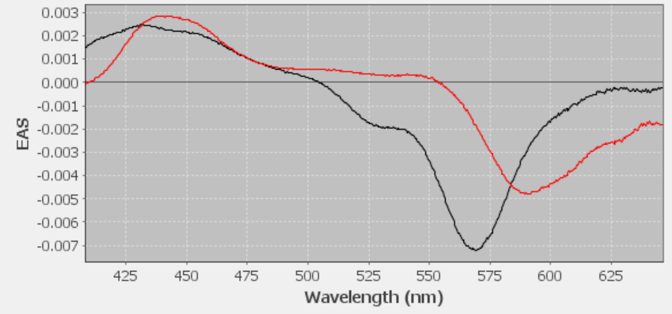

Figure S26: EAS of **O-Th** in MeCN. Red = 6.25 ps, Black = 1044 ps

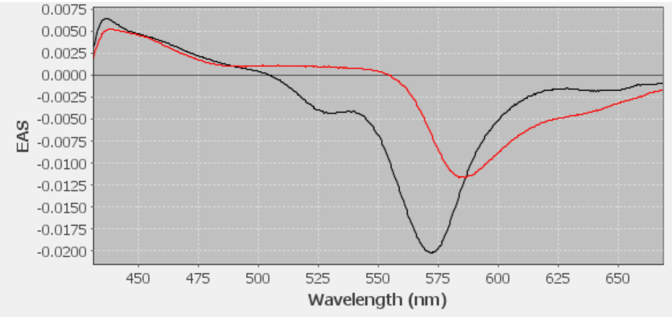

Figure S27: EAS of **O-Th** in CH_2Cl_2 . Red = 6.8 ps, Black = 2674 ps

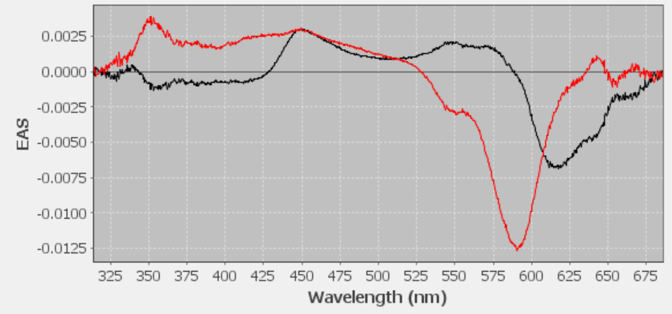

Figure S28: EAS of **S-Th** in MeCN. Black = 38 ps, Red = 105 ps

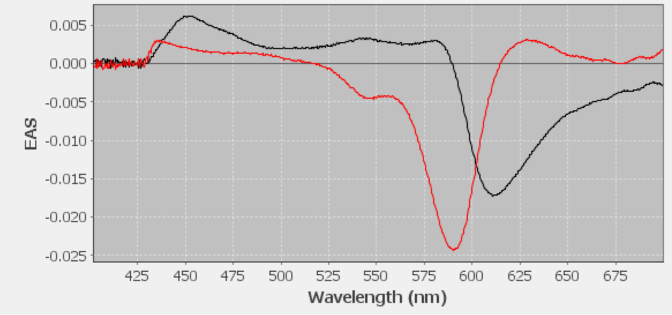

Figure S29: EAS of **S-Th** in CH_2Cl_2 . Black = 56 ps, Red = 195 ps

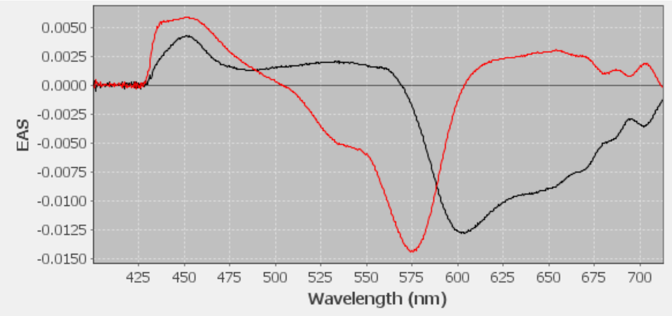

Figure S30: EAS of **O-Th-5-CO$_2$H** in acidified MeCN. Black = 7.4 ps, Red = 118 ps

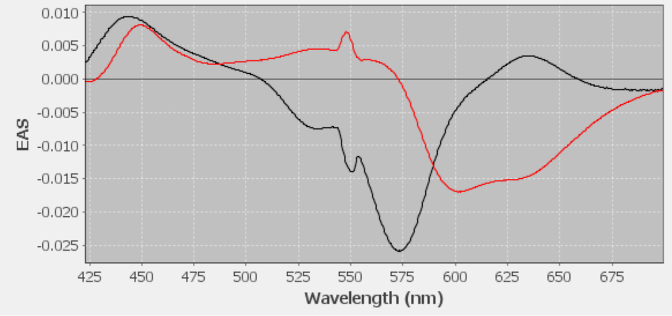

Figure S31: EAS of **O-Th-5-PO(OEt)$_2$** in MeCN. Red = 13.5 ps, Black = 247 ps

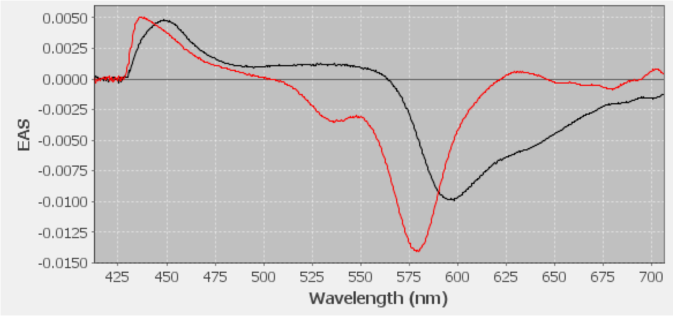

Figure S32: EAS of **O-Th-5-PO(OEt)$_2$** in CH_2Cl_2 . Black = 13.0 ps, Red = 736 ps

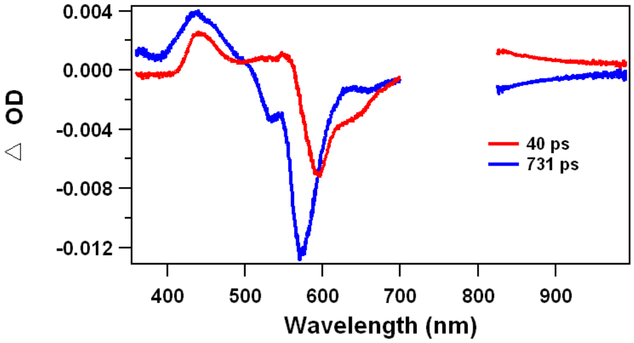

Figure S33: EAS of **O-Th** in 1:1 (v:v) methanol and glycerol mixture.

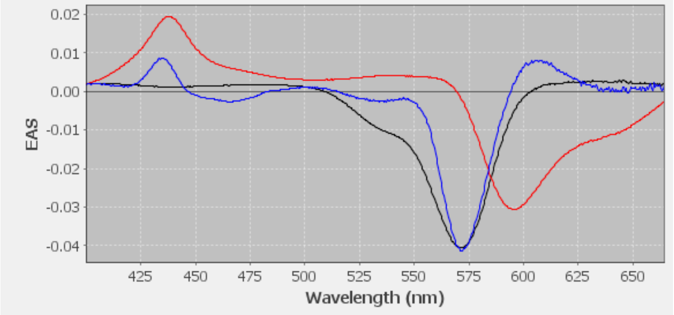

Figure S34: EAS of **Se-Pyr** in MeCN. Blue = 0.1 ps, Red = 79.5 ps, Black = triplet state

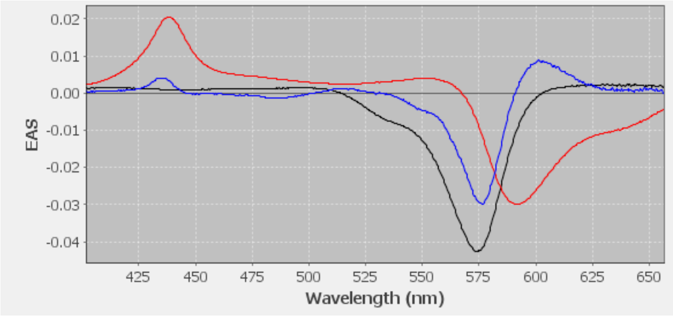

Figure S35: EAS of **Se-Pyr** in CH_2Cl_2 . Blue = 0.2 ps, Red = 51.1 ps, Black = triplet state

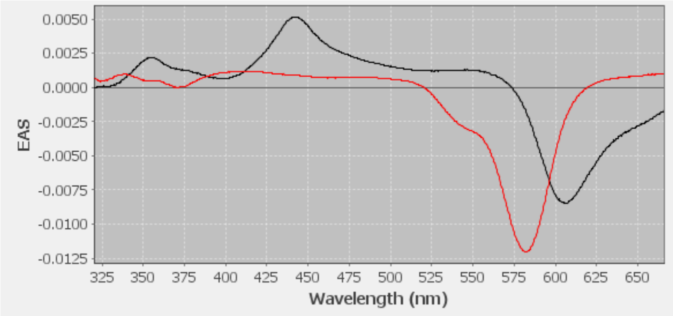

Figure S36: EAS of **Se-Ph** in MeCN. Black = 53 ps, Red = Triplet State

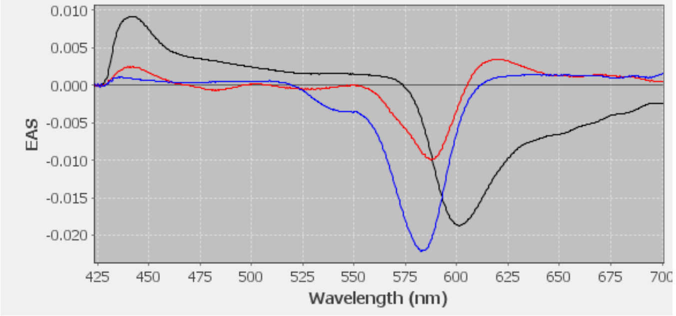

Figure S37: EAS of **Se-Ph** in CH_2Cl_2 . Red = 0.5 ps, Black = 35 ps, Blue = Triplet State

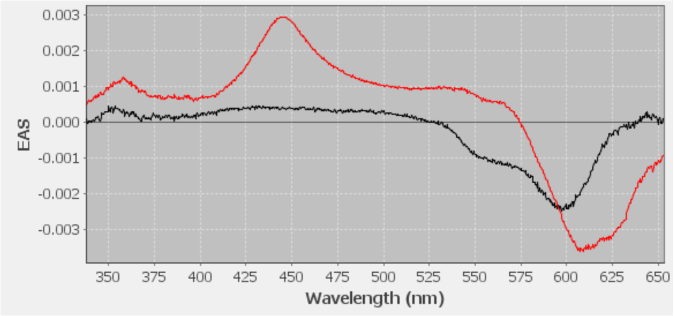

Figure S38: EAS of **Se-Th** in MeCN. Red = 29 ps, Black = triplet state

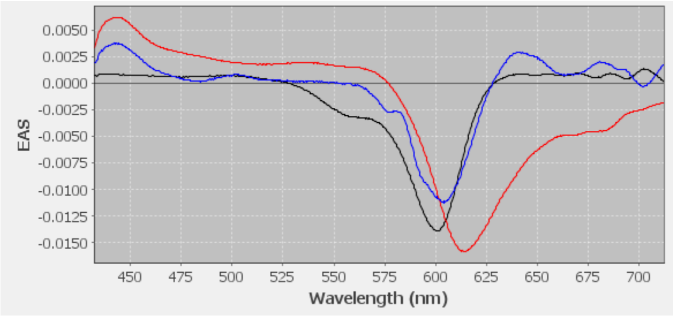

Figure S39: EAS of **Se-Th** in CH_2Cl_2 . Blue = 0.2 ps, Red = 26 ps, Black = triplet state

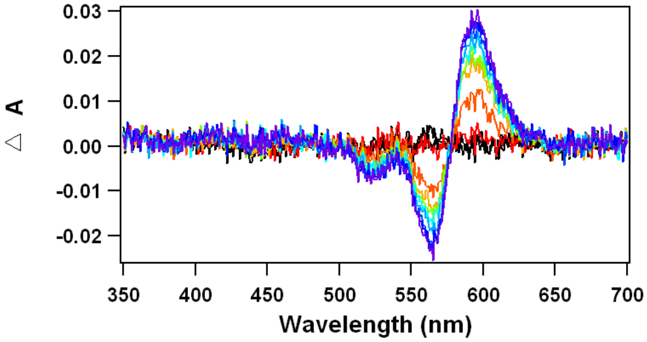

Figure S40: Spectroelectrochemistry of **O-Th**. The spectrum of the ground state absorption was subtracted as a background. No change in the spectrum was recorded at potentials less positive than the oxidation potential (black curves). A positive peak then grows in to the red of the ground state bleach.

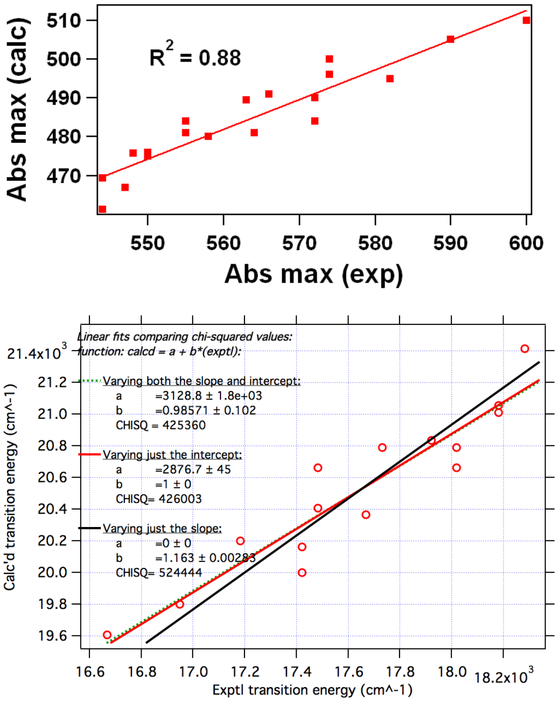

Figure S41: Linear least squares fit of calculated absorption wavelengths versus experimental absorption wavelengths (top) and linear fits of the calculated versus experimental transition energies (bottom). In (a), the coefficient of determination, R^2=0.88, indicates a strong correlation across the set of compounds. The calculated vs experimental energy regressions show that the TD-DFT calculated energy is consistently 2877 ± 45 cm^{-1} above the observed energy of the absorption band. Note that there is a negligible improvement in the chi-squared value when both the slope and intercept are varied versus when just the intercept is varied.

Table S2: HOMO Energies and Fragment Contributions.

		HOMO Fragment Contributions				
Dye	**HOMO Energy (eV)**	Chalcogen	9 position	Amino groups	Aryl	Xanthene Core (excluding C-9)
O-Pyr	-5.96			0.42	N/A	0.57
S-Pyr	-5.96			0.43	N/A	0.57
Se-Pyr	-5.96			0.42	N/A	0.57
O-Ph	-5.96			0.43		0.57
S-Ph	-5.96			0.43		0.57
Se-Ph	-5.96			0.42		0.57
O-Th	-5.96			0.43		0.57
S-Th	-5.98			0.43		0.57
Se-Th	-5.96			0.42		0.57
O-Ph-*o*-CO_2H	-5.96			0.43		0.57
O-Ph-*o*-CO_2^-	-5.77			0.42	0.01	0.56
O-Ph-*p*-CO_2H	-5.98			0.43		0.57
O-Ph-*p*-CO_2^-	-5.90			0.43		0.57
O-Th-2-CO_2H	-5.97			0.43		0.57
O-Th-2-CO_2^{--}	-5.82			0.42		0.57
O-Th-5-CO_2H	-6.01			0.43		0.56
O-Th-5-CO_2^-	-5.90			0.43		0.57

Table S3: LUMO Energies and Fragment Contributions

		LUMO Fragment Contributions				
Dye	**LUMO Energy (eV)**	Chalcogen	9 position	Amino groups	Aryl	Xanthene Core (excluding C-9)
O-Pyr	-3.10	0.04	0.29	0.14	N/A	0.53
S-Pyr	-3.16	0.09	0.28	0.14	N/A	0.49
Se-Pyr	-3.18	0.09	0.29	0.14	N/A	0.48
O-Ph	-3.16	0.04	0.27	0.13	0.05	0.51
S-Ph	-3.21	0.09	0.28	0.13	0.02	0.49
Se-Ph	-3.24	0.09	0.28	0.13	0.02	0.48
O-Th	-3.24	0.04	0.26	0.13	0.09	0.49
S-Th	-3.32	0.09	0.27	0.13	0.03	0.48
Se-Th	-3.35	0.09	0.27	0.13	0.03	0.47
O-Ph-*o*-CO_2H	-3.16	0.04	0.26	0.13	0.03	0.55
O-Ph-*o*-CO_2^-	-2.80	0.04	0.27	0.12	0.05	0.53
O-Ph-*p*-CO_2H	-3.29	0.04	0.24	0.12	0.13	0.47
O-Ph-*p*-CO_2^-	-3.10	0.04	0.27	0.13	0.06	0.51
O-Th-2-CO_2H	-3.21	0.04	0.26	0.13	0.03	0.54
O-Th-2-CO_2^{--}	-2.96	0.04	0.27	0.13	0.03	0.53
O-Th-5-CO_2H	-3.45	0.04	0.21	0.11	0.20	0.43
O-Th-5-CO_2^-	-3.18	0.04	0.26	0.12	0.10	0.48

Table S4: LUMO + 1 Energies and Fragment Contributions.

		LUMO+1 Fragment Contributions				
Dye	**LUMO+1 Energy (eV)**	Chalcogen	9 position	Amino groups	Aryl	Xanthene Core (excluding 9 position)
O-Pyr	-1.09			0.03	N/A	0.96
S-Pyr	-1.28	0.01		0.03	N/A	0.95
Se-Py	-1.20	0.02		0.03	N/A	0.94
O-Ph	-1.14		0.06	0.02	0.11	0.81
S-Ph	-1.33	0.01		0.03	0.12	0.84
Se-Ph	-1.28	0.02		0.03	0.15	0.81
O-Th	-1.25				0.72	0.28
S-Th	-1.31	0.01		0.05		0.94
Se-Th	-1.22	0.02		0.04	0.01	0.93
O-Ph-*o*-CO_2H	-2.12				0.99	0.02
O-Ph-*o*-CO_2^-	-1.12				0.80	0.20
O-Ph-*p*-CO_2H	-2.04		0.03	0.01	0.85	0.1
O-Ph-*p*-CO_2^-	-1.17				0.82	0.17
O-Th-2-CO_2H	-2.30				0.98	
O-Th-2-CO_2^{--}	-1.26				0.87	0.12
O-Th-5-CO_2H	-2.28		0.04	0.02	0.80	0.14
O-Th-5-CO_2^-	-1.39				0.82	0.18

Table S5: Hammett constants of Aryl Substituents

Substituent	σ_m	σ_p	σ_p^+	σ_p^-
C_5H_6	0.06[4]	-0.01[4]	-0.18[5]	0.02[6]
2-thienyl (as in Th, Th-5-R)	0.09[7]	0.05[7]	-0.43[8]	0.19[7]
3-thienyl (as in Th-2-R)	0.03[7]	-0.02[7]	-0.38[8]	0.13[7]

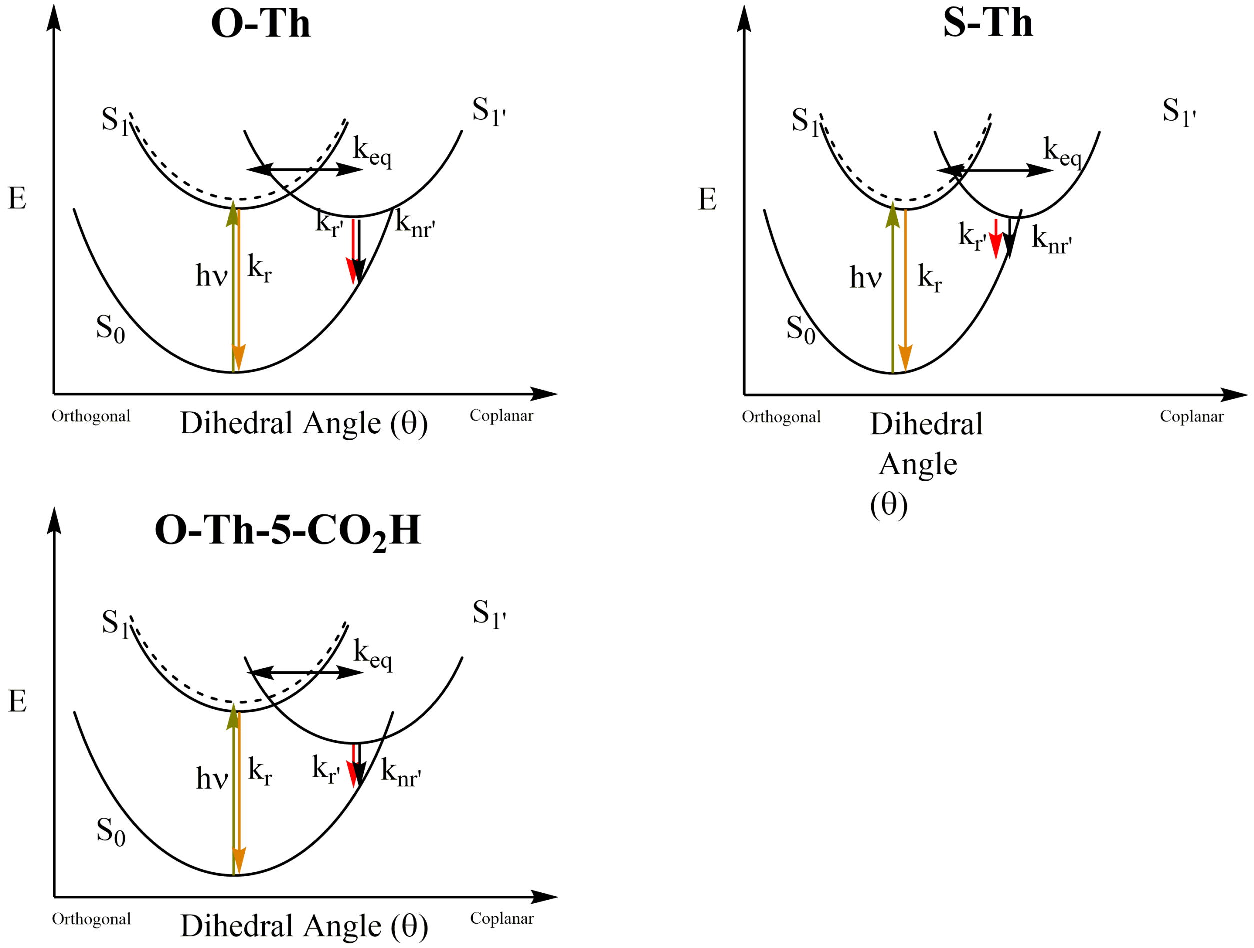

Figure S42: Energy level diagrams suggesting an explanation for the much faster fluorescence lifetimes of **S-Th** and **O-Th-5-CO$_2$H**. Compared to **O-Th**, **S-Th** exhibits more restriction on torsion about the thienyl – xanthylium bond, resulting in steeper potential wells. This rapid rise in the ground-state energy as the aryl group rotates in the excited state could significantly decrease the $S_{1'}$-S_0 energy gap, increasing the rate of $k_{nr'}$, and decreasing the lifetime and fluorescence quantum yield. For **O-Th-5-CO$_2$H**, the electron withdrawing group on the thienyl likely lowers the energy of $S_{1'}$, causing a faster rate of nonradiative decay, $k_{nr'}$. Hence for **S-Th** and **O-Th-5-CO$_2$H**, the "k_{eq}" process would be better described as a unidirectional relaxation to $S_{1'}$ with the concomitant loss of fluorescence from S_1.

Preliminary Hydrogen Production Experiments

Preliminary photochemical experiments leading to H_2 generation were conducted to assess the acid versions of **O-Ph-*p*-PO(OEt)$_2$** and **O-Th-5-PO(OEt)$_2$** as sensitizers. Platinized titanium dioxide (Pt-TiO_2) was prepared as previously reported.[9] 10 mg of 0.5% Pt-TiO_2 was placed in each of 40 mL vials. From a 1:3 MeCN:H_2O stock solution of the dye with an absorbance of 0.8 in a 2-mm cuvette, 2.5 mL was placed in each reaction vial. Using a fixed absorbance instead of concentration of the stock dye solution eliminates errors in calculating the molar absorptivity, ε, and ensures that the samples absorb equivalent amounts of light. The solution of dye (as photosensitizer) and Pt-TiO_2 were sonicated for two minutes. 2.5 mL of a 0.2 M ascorbic acid solution (pH = 4) was then added, making the ${}^{s}_{s}pH = 5.1$ for the final solution.[10] The final dye solutions were therefore approximately 25 μM. Under these conditions, strong binding of the dye onto TiO_2 has been shown in prior studies using the phosphonic acid anchor.[11] Reaction solutions were then transferred to the photolysis apparatus (described previously[11]) and degassed at 15° C for 20 minutes. Samples were then illuminated with white LED light while hydrogen production was monitored via pressure transducers in the headspace of the vials. Hydrogen production was corroborated by GC analysis of the headspace gas.

As displayed in Figure S43, systems containing **O-Ph-*p*-PO(OEt)$_2$** or **O-Th-5-PO(OEt)$_2$** appear to be very similar in terms of activity despite **O-Ph-*p*-PO(OEt)$_2$** having an almost ten times longer excited state lifetime.

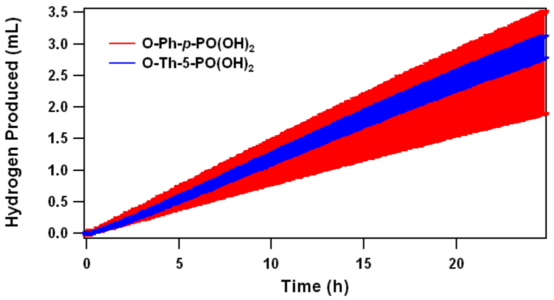

Figure S43: Hydrogen production of **O-Ph-*p*-PO(OH)$_2$** and **O-Th-5-PO(OH)$_2$** using 1:3 MeCN:H_2O with 0.1 M ascorbic acid (${}^{s}_{s}pH = 5.1$) and 0.5% Pt-TiO_2 as catalyst. Error bars are shown to indicate uncertainty in measurement. The deviation in activity of **O-Ph-*p*-PO(OEt)$_2$** was larger than for **O-Th-5-PO(OEt)$_2$**, potentially due to poorer solubility in the solvent mixture before attachment.

References:

(1) Del Valle, D. J., Donnelly, D. J., Holt, J. J. and Detty, M. R. "2,7-Bis-N,N-Dimethylaminochalcogenoxanthen-9-Ones Via Electrophilic Cyclization with Phosphorus Oxychloride" *Organometallics* **2005**, *24,* 3807-3810
(2) Mulhern, K. R., Orchard, A., Watson, D. F. and Detty, M. R. "Influence of Surface-Attachment Functionality on the Aggregation, Persistence, and Electron-Transfer Reactivity of Chalcogenorhodamine Dyes on Tio2" *Langmuir* **2012**, *28,* 7071-7082
(3) Spek, A. "Structure Validation in Chemical Crystallography" *Acta Crystallographica Section D* **2009**, *65,* 148-155
(4) McDaniel, D. H. and Brown, H. C. "An Extended Table of Hammett Substitutent Constants Based on the Ionization of Substituted Benzoic Acids" *J. Org. Chem.* **1958**, *23,* 420-427
(5) Brown, H. C. and Okamoto, Y. "Electrophilic Substituent Constants" *J. Am. Chem. Soc.* **1958**, *80,* 4979-4987
(6) Litvinenko, L. M. "Structure and Reactivity of Aromatic Amines" *Bulletin of the Academy of Sciences of the USSR, Division of chemical science* **1962**, *11,* 1653-1661
(7) Fringuelli, F., Marino, G. and Taticchi, A. "Heteroaromatic Rings as Substituents. Part I. Evaluation of [Sigma]- and [Sigma]--Constants of 2- and 3-Thienyl Groups" *Journal of the Chemical Society B: Physical Organic* **1970**, 1595-1598
(8) Fringuelli, F., Marino, G. and Taticchi, A. "Heteroaromatic Rings as Substituents. Part Ii. Evaluation of the Electrophilic Substituent Constants for 2- and 3-Thienyl Groups from the Solvolysis of 2-Chloro-2-(Thienylphenyl)Propanes in 90% Aqueous Acetone" *Journal of the Chemical Society B: Physical Organic* **1971**, 2302-2303
(9) Zheng, B., Sabatini, R. P., Fu, W.-F., Eum, M.-S., Brennessel, W. W., Wang, L., McCamant, D. W. and Eisenberg, R. "Light-Driven Generation of Hydrogen: New Chromophore Dyads for Increased Activity Based on Bodipy Dye and Pt(Diimine)(Dithiolate) Complexes" *Proc. Natl. Acad. Sci.* **2015**, *112,* E3987-E3996
(10) Espinosa, S., Bosch, E. and Rosés, M. "Retention of Ionizable Compounds on Hplc. 5. Ph Scales and the Retention of Acids and Bases with Acetonitrile−Water Mobile Phases" *Anal. Chem.* **2000**, *72,* 5193-5200
(11) Sabatini, R. P., Eckenhoff, W. T., Orchard, A., Liwosz, K. R., Detty, M. R., Watson, D. F., McCamant, D. W. and Eisenberg, R. "From Seconds to Femtoseconds: Solar Hydrogen Production and Transient Absorption of Chalcogenorhodamine Dyes" *J. Am. Chem. Soc.* **2014**, *136,* 7740-7750